

Analysis of ballistic impact performance and shear effect on elastomeric and thermoset composites

Seyedeh Samaneh Asemani^a, Gholamhossein Liaghat^{a,b,*}, Hamed Ahmadi^a, Yavar Anani^a, Sahand Chitsaz Charandabi^c, Amin Khodadadi^a

^aDepartment of Mechanical Engineering, Tarbiat Modares University, Tehran, Iran

^bSchool of Mechanical & Aerospace Engineering, Kingston University, London, England, United Kingdom

^cSchool of Mechanical Engineering, Coventry University, England, United Kingdom

*Corresponding author. E-mail addresses: Ghlia530@modares.ac.ir and G.Liaghat@kingston.ac.uk (Gh. Liaghat)

The present study proposes a new theoretical model for high-velocity impact in two kinds of target, kevlar/elastomer and kevlar/epoxy composites, and comprehensively discusses and compares these. In this analysis, with the aid of hyperelasticity theory, energy absorption equations are derived based on the linear and nonlinear behaviour of constituents to assess the dependence of the ballistic limit on the interaction of the first, second, third, and fourth layers of the laminate on each other. Furthermore, to investigate the matrix effect on the in-plane shear, tensile tests were performed at $\pm 45^\circ$ direction for both kevlar/elastomer and kevlar/epoxy composite laminates. The results indicate that the adhesion of kevlar fibers to the rubber matrix is more substantial than their adhesion to the epoxy matrix, increasing the failure shear strain of elastomeric composites and reducing the debonding between the fiber and the matrix which led to greater ballistic velocity. The results of the experimental tests verified the proposed model and confirmed its precision. With this verified model, the thickness effect on the ballistic behaviour of the targets was investigated.

Keywords: Theoretical impact analysis; high-velocity impact; absorbed energy; kevlar fabric; elastomeric composite.

1. Introduction

Generally, problems of impact in the past were mainly of military concern in developing armor or ammunition for either defensive or offensive purposes. Nowadays, increasing demands from civilian applications concern the safety of the products; therefore, it is necessary to know about the behaviour of materials under intense brief pressure or impact loading [Benzait and Trabzon, 2018].

[Naik, 2016] studied ballistic materials to protect personnel and structures against projectiles and explosives. In his formulation, measured conical deformation and the kinetic energy carried by a cone-formation on the back face of a target are presented. [Naik and Doshi, 2008] also investigated the behaviour of thick woven fabric composites under ballistic impact. The method that was established by them was based on energy balance. It detected that shear plugging is the principal mechanism of energy absorption. During the last few decades, the ballistic resistance of materials and their ability to absorb energy have been widely studied through experiments and analytical methods [Yang and Chen, 2016; Mahesh et al., 2021; Ahmadi and Liaghat, 2019]. [Kumar et al., 2010],

using numerical simulations, investigated the ballistic response to cylindrical projectiles and absorbed energy by thick Kevlar/epoxy composite plates. [Ahmadi et al., 2011] presented the influence of thickness on the high velocity impact of FMLs experimentally and numerically. [Mamivand et al., 2010] considered the effect of a target's dimensions on its ballistic performance in an analytical model that could be used for optimizing the structure of armor. [Pol et al., 2015] investigated the behaviour of two-dimensional woven glass/epoxy/nanoclay nanocomposites under ballistic impact and the absorbed energy by using a theoretical model for each time interval.

Despite the motivating mechanical properties of thermoset (TS) resin in high-performance composite materials, it has an undesirable effect on the fabric because it makes the composite hard and inflexible. Therefore, to have flexible composites, other polymer matrices must be considered. One of the oldest materials in the engineering applications is elastomers. Natural rubber can be used instead of the TS matrix while preserving composite flexibility. Rubbers are extensively used in shock absorbers, impact resistance panels, and other engineering applications [Khodadadi et al., 2019; Yang et al., 2018; Tubaldi et al., 2018]. The most distinguishing property of elastomers is their capacity to endure large deformations under comparatively small stresses and maintain their initial shape without significant permanent deformation after unloading [Thiruvarudchelvan, 1993; Brinson and Brinson, 2008]. Neo-Hookean, Mooney-Rivlin, Ogden, Yeoh, Arruda-Boyce and Vander Waals models were investigated for strain energy functions by using data on uniaxial tension, and compression. It was observed that the proposed model of stored energy function gives a better estimation for tension and compression test for strains less than 50% [Ng et al., 2011].

Previous studies predicted analytical models for behaviour and energy absorption under ballistic impact loading on single-layer composites [Naik and Doshi, 2008]. Hence, these models were extended for multi-layer composites according to the central assumption that the energy absorption of different layers was considered independently of each other. Consequently, the analytically predicted results have differed from the experimental results.

In the present paper, the interaction between the layers are considered. This makes the energy absorption of the layers wholly interdependent by specifying the strain in the thickness direction in terms of length to more accurately describe the ballistic impact on the composite target. The high-velocity impact resistance of kevlar/elastomer and kevlar/epoxy composites is also investigated, and the energy absorption of these two composites is compared.

Furthermore, a comprehensive analytical formulation was developed based on hyperelasticity relationships, for the behaviour of a kevlar/elastomer composite under the ballistic impact of a spherical ended cylindrical projectile. Tensile tests were performed to investigate the in-plane shear matrix effect at $\pm 45^\circ$ laminates on kevlar/elastomer and kevlar/epoxy composites. Finally, the ballistic impact behaviour of composites was theoretically validated by uniaxial experimental results from Ref. [Khodadadi et al., 2019].

2. Analytical formulation

The presented analytical model was established on the basis of energy balance. The purpose of this analytical primary formulation was to calculate the absorbed energy for different failure mechanisms and the ballistic limit velocity for different ranges of laminate thicknesses. This section uses an analytical model of stress wave diffusion and energy balance between a rigid cylindrical projectile and a multi-layer target. The primary features of the model are:

- (i) During penetration, the projectile is rigid and undeformed,
- (ii) During penetration in each time interval, the motion of the projectile is uniform,
- (iii) The projectile is a cylinder with a spherical end,
- (iv) The maximum strain of a layer in the transverse direction is the initial strain on the next layer,
- (v) Energy absorption of primary yarn/fiber breakage, and secondary yarns deformation act independently,
- (vi) In all of the layers, the longitudinal and transverse wave velocities are the same,
- (vii) During penetration in any time interval, the velocity of the projectile remains constant,
- (viii) The interval time is obtained with the displacement and velocity at the end of each layer composite,
- (ix) In all of the layers composite, the difference between the initial and final strains is uniform,
- (x) In all of the layers composite, the shear plugging stress is uniform, and friction is neglected.

To determine the energy absorbed by the target for the various structural types of these materials their stress formulas were calculated separately.

2.1. Energy-absorbing mechanisms

The analytical model in the present study reproduced the expected effects of rigid projectiles against the kevlar/elastomer and kevlar/epoxy composites when struck by a projectile. Shear plugging on the front face and cone formation on the back face start depending on the target material properties during the ballistic impact event. It is assumed that the velocity of the moving cone is the same as the projectile's velocity. Initially, the moving cone has velocity equal to that of the projectile and has zero mass. As time progresses, the mass of the cone increases and the velocity of the cone decreases. As the cone formation takes place, the yarns/fibers deform and absorb some energy. The primary yarns which provide the resistive force to the projectile motion are strained the most, thus leading to their failure. When all the primary yarns fail, the projectile exits the target. Failure yarns, therefore, absorbs some energy of the projectile. Delamination and matrix cracking occurs in the laminate area during the ballistic impact event and the cone is formed, as explained earlier. Various components of absorbed energy after the projectile impacted the composite target can be shown in the energy balance equation as the following:

$$E_{Kp,i-1} = E_{Kp,i} + E_{KE,i} + E_{Py,i} + E_{Sy,i} + E_{Dl,i} + E_{Mc,i} + E_{Sp,i} \quad (2.1)$$

where $E_{Kp,i-1}$ is the initial kinetic energy of the projectile, $E_{Kp,i}$ is the kinetic energy of the projectile at each time-step, $E_{KE,i}$ is the kinetic energy of the composite cone in front of the projectile tip, $E_{Py,i}$ is the energy absorbed by the primary yarn, $E_{Sy,i}$ is the energy absorbed by the secondary yarn, $E_{Dl,i}$ and $E_{Mc,i}$ are the energies absorbed by the delamination between the layers and the matrix cracking and $E_{Sp,i}$ is the energy dissipated by the layers plugging. The total energy absorbed by the target is considered in Eq. (2.2):

$$E_{L,i} = E_{Py,i} + E_{Sy,i} + E_{Dl,i} + E_{Mc,i} + E_{Sp,i} \quad (2.2)$$

Hence, during the ballistic impact, the velocity of the projectile at the end of i th time interval is given by:

$$V_i = \sqrt{\left(\frac{1}{2} m_p V_0^2 - E_{L,i}\right) / \frac{1}{2} (m_p + m_{c,i})} \quad (2.3)$$

where $m_{c,i}$ is the mass of the moving conoid at time t_i . Since ballistic impact takes place in a high-velocity event by a low-mass projectile, only the damage effects on the target can be seen at the point of impact, followed by the transfer of energy during penetration from the projectile to the target. The following assumptions were made in the analytical formulation for the properties of the target material and the parameters of the projectile:

- 1) It shows that the primary energy of the projectile is greater than the energy absorbed by the target when the projectile makes a hole in the target, and the complete perforation takes place. Here, the projectile exits with a residual velocity.
- 2) In other cases, when the primary energy of the projectile is less than the energy absorbed by the target, the projectile must have incompletely penetrated the target, or the projectile has become stuck in the target.
- 3) It shows that the target has absorbed the total energy of the projectile when the projectile makes a hole in the target and exits with zero velocity.

The various mechanisms of energy-absorbing should be precise for the full understanding of ballistic impact into composites. This model's potential energy-absorbing tools are:

- Cone-formation on the back face of the target.
- Deformation of secondary yarns.
- Tension in primary yarns/fibers.
- Delamination.
- Matrix cracking.
- Shear plugging between the projectile and the target.
- In multiple materials such as carbon, glass, or kevlar, various mechanisms may dominate. Reinforcement construction may influence the means of absorbing energy.

2.1.1. Cone-formation on the back face of the target

Transverse ballistic impact on a composite target causes the layers to be compressed, and shear stress waves were observed through the thickness of the laminate and tensile, together with shear stress waves in the in-plane direction [Meyers, 1994]. Previous research using high-velocity photography indicated that a cone was formed on the back face of the composite as the ballistic impact took place [Guoqi et al., 1992; Bresciani et al., 2015].

Fig. 1 shows the deformation and cone-formation on the back face of the composite during permeation by advancing the projectile in the direction of thickness. In the present study, the head of the projectile was considered to be spherical. Here, d_p is the projectile diameter, x_{ii} is the cone-shaped surface radius, and h_i is the permeation depth in the composite thickness. The depth of the cone formation and the distance travelled by the projectile are equal during permeation. In addition, the projectile velocity and the moving cone would have been identical. Along the yarn, the longitudinal/radial propagation of the stress wave takes place on the target plate plane. The shape of the stress wave front on the target plane is circular. The surface radius of the cone formed can be calculated on the basis of transverse wave propagation. The primary yarns are the yarns in a straight line below the projectile. These yarns provide the resistant force to the penetration of the projectile into the target. These yarns also deform and absorb some amount of energy. The secondary yarns are the residual yarns within the conical region. These yarns cause some energy to be absorbed [Naik, 2016].

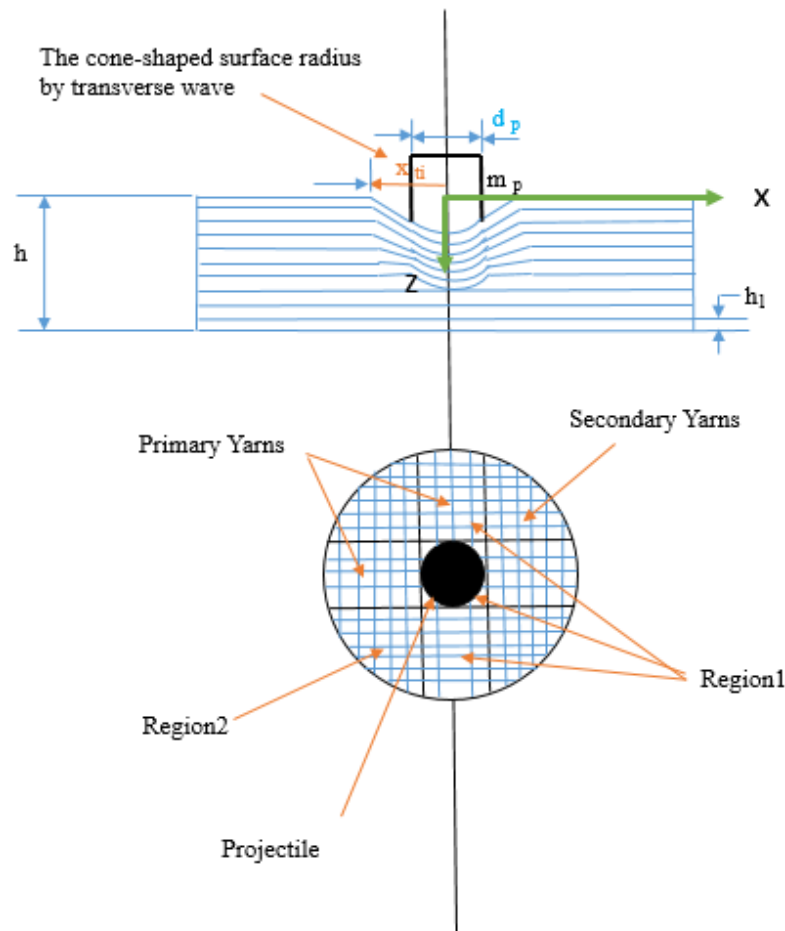


Fig. 1. Propagation of damage in composite during ballistic impact: tensile and compression deformed side and front view.

A completed ballistic impact incident can be divided into many small intervals. Hence, at the i th interval t_i , $r_{i,i}$ is the distance that the transverse wave has travelled. This can be considered by

$$r_{i,i} = \sum_{t=0}^{i=n} r_t \left(\frac{h_i}{h} \right) \quad (2.4)$$

At first, the in-plane longitudinal and transversal waves propagate in the first layer, and the in-thickness longitudinal wave starts propagating. The first layer undergoes the cone (V-tent) deformation as the projectile advances, while the rear layers remain undeformed. When the wave reaches a new layer, the hypothesis is made that in-plane transversal and longitudinal waves propagate in that layer. When through thickness longitudinal wave reach to a new layer, it starts moving along the penetration direction at the same speed as the previous layer pushing it. In turn, it starts pushing the following layer that is still undeformed. Therefore, every layer consecutively undergoes the formation of the cone deformation, which induces strain in the yarns, as described below. This mechanism continues until the wave reaches the rearmost layer. From that moment on, all the layers move at the projectile's speed and undergo strain and stress leading to possible failure. The longitudinal wave reflects from the rear free surface, but the physical effects of this phenomenon are neglected in this model. In a fixed coordinate system, the steps of the mechanism described in Fig. 2.

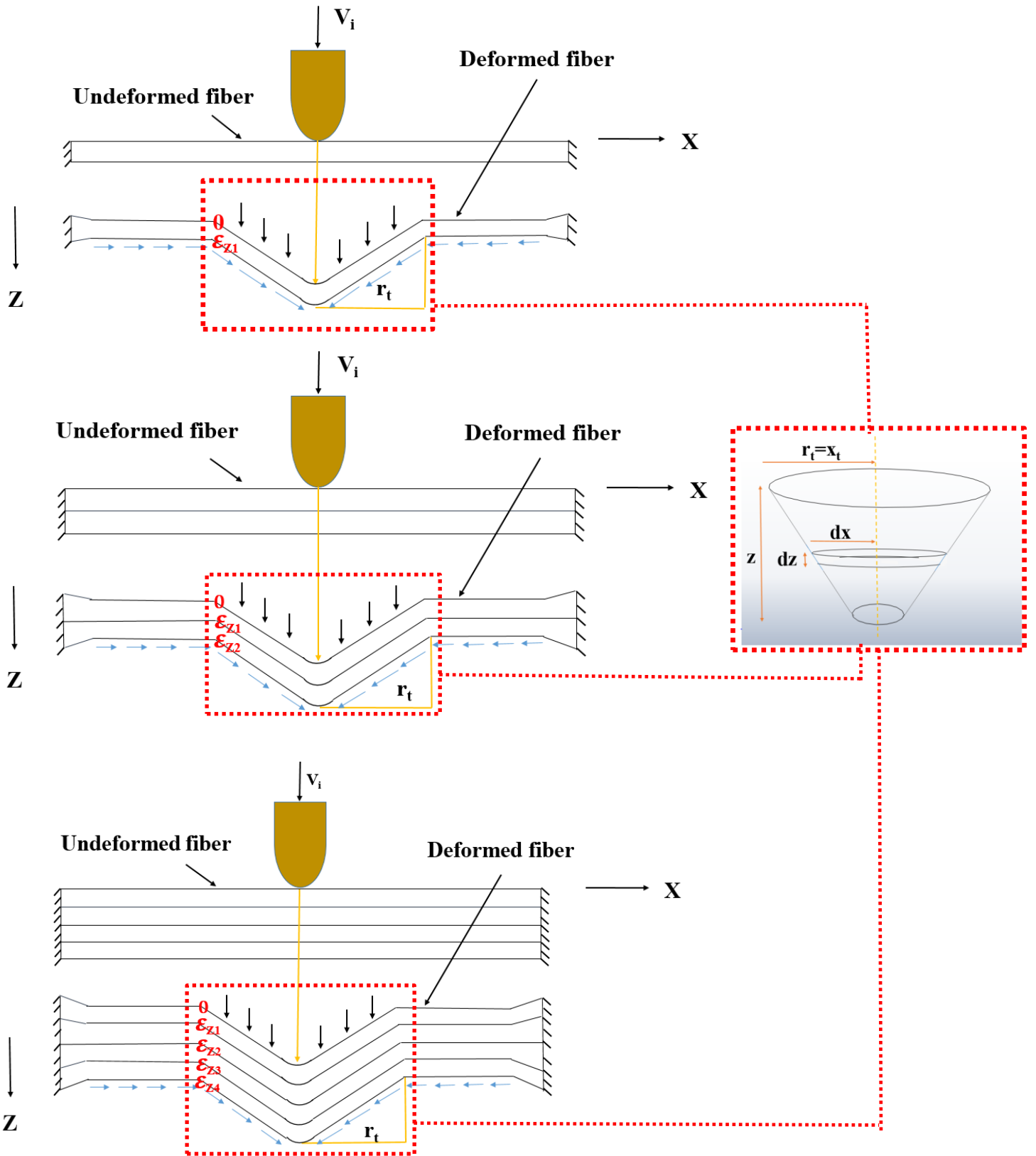


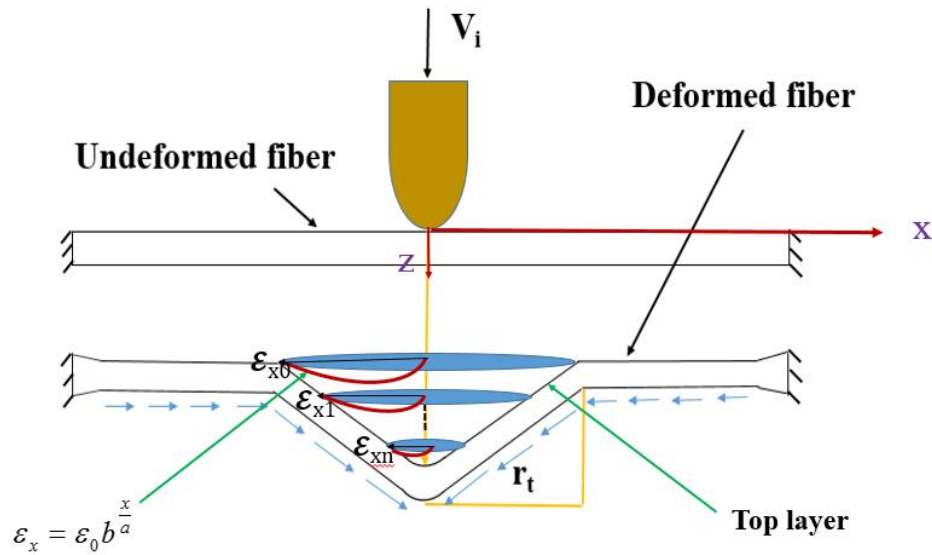
Fig. 2. A yarn/fiber configuration before and after impact: (a) 1-layer, (b) 2-layer and (c) 4-layer.

According to Figs.3a and 3b, the longitudinal strain on each layer surface depends on the transverse radius of the cone and is shown as power [Naik, 2006]. Also, the transverse wave causes a strain in the thickness direction, the value of which varies with the maximum amount of transverse radius at each level of each layer. It should be noted that for composite targets under the impact of a hemispherical projectile, the damaged surface is an incomplete cone with a projectile diameter on the front surface and a generating angle of 45° [Pandya, 2012] (Fig. 3c). According to the hypotheses presented in the previous section, the velocity of longitudinal and transverse waves is the same in all layers. The difference in longitudinal strain across all layers with the same transverse radius is constant at the end of the time interval. The difference between the output and input strains is the same in all layers in the longitudinal and transverse directions. Therefore, in the 1- layer, the strain difference in the longitudinal direction (x) with the strain difference in the transverse direction (z) is assumed by:

$$\varepsilon_{z1} - 0 = \varepsilon_{x0} - 0 \rightarrow \varepsilon_{z1} = \varepsilon_{x0} \quad (2.5)$$

Thus, the strain difference of other layers in the transverse direction (z) such as 2- layer, 3- layer, 4 –layer, ..., n –layer is calculated as follows:

$$\varepsilon_{z2} = 2\varepsilon_{z1}, \varepsilon_{z3} = 2\varepsilon_{z2}, \dots, \varepsilon_{zn} = 2\varepsilon_{z(n-1)} \quad (2.6)$$



(a)

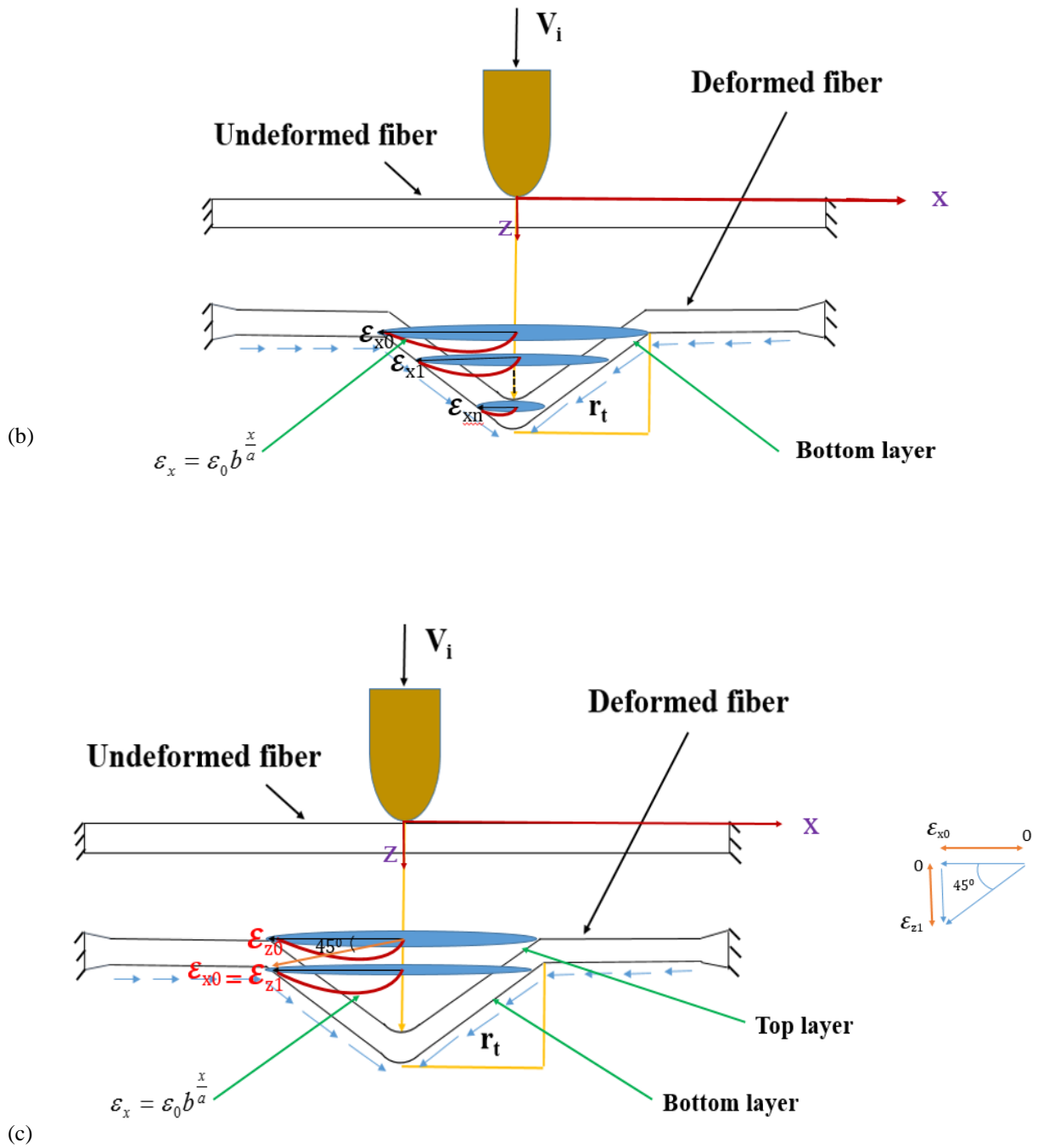


Fig.3. (a) Longitudinal strain in terms of the transverse radius of primary fibers at the top surface of the 1- layer, (b) longitudinal strain in terms of the transverse radius of primary fibers at the bottom surface of the 1- layer and (c) Transverse strain in terms of the longitudinal strain at the top and bottom of the 1- layer.

2.1.2. Energy absorption of the moving cone formation

During the ballistic impact, V_i is the projectile velocity at the end of the i th time interval, which is equal to the cone-shaped portion velocity of the target. Hence, the energy absorption of the cone formation at the end of the i th time interval is

$$E_{KE,i} = \frac{1}{2} m_{c,i} V_i^2, \quad m_{c,i} = \pi r_{t,i}^2 h_i \rho \quad (2.7)$$

2.1.3. Energy absorption of the failure of primary yarns(Region 1) under projectile pressure

As the transverse wave propagates in the thickness direction, compression of the target takes place in region 1, where all of the primary yarns fail at the same time in one layer composite (Fig. 1). The projectile displacement results in transverse strain in the layers by the transverse wave. Hence, the general energy absorbed equation due to projectile pressure in Region 1 is as follows:

$$E_{py,i} = \sum_{i=1}^{i=n} A \int_0^{r_{t,i}} \left(\sum_{i=0}^{i=n-1} \int_{\varepsilon_{zi}^* = i \varepsilon_0 b^a}^{\varepsilon_{z(i+1)} = (i+1) \varepsilon_0 b^a} \sigma_z(\varepsilon) d\varepsilon \right) dx \quad (2.8)$$

where ε_0 is the limit of ultimate strain, b is the factor of transmission, a is the width of yarn, and $A = 4d_p h_1$. The stresses for elastic (linear) materials and hyperelastic (nonlinear) materials in Eq. (2.8) are discussed below.
1) The stress in a single direction for elastic (linear) materials based on strain is as follows:

$$\sigma_z = E \varepsilon_z \quad (2.9)$$

2) The stress in one direction in hyperelasticity is not considered to be due directly to strain, as in small strains of linear elastic materials. In general, the strain energy density function W in hyperelastic material is a function of the stretch invariants of the deformation gradient tensor F . The right Cauchy-Green tensor $C = F^T F$ and the left Cauchy-Green tensor $B = F F^T$ are often easier to estimate. The Lagrangian strain tensor is assumed by $2E = (C - I)$, where I is the identity matrix. Isotropic materials (e.g., rubbers) can indicate strain energy function (SEF) in terms of the right (or left) Cauchy Green tensor C (or B) invariants (I_1, I_2, I_3) or eigenvalues of deformation gradient tensor F , defined principal stretches ($\lambda_1, \lambda_2, \lambda_3$) [Ogden, 2003]. For rubber material, the incompressibility hypothesis $I_3 = 0$ is often used. The fundamental relation for materials of hyperelastic is [Ogden, 2003]:

$$S = 2 \left(\frac{\partial W}{\partial I_1} I + \frac{\partial W}{\partial I_2} (I_1 I - C) + \frac{\partial W}{\partial I_3} I_3 C^{-1} \right) \quad (2.10)$$

The second Piola-Kirchhoff stress transformation to Cauchy stress tensor σ gives [Ogden, 2003] $\sigma = 2F(\partial W / \partial C)F^T \rightarrow \sigma = (1/J)FSF^T$ where $J = \det F$. Furthermore, for incompressible materials like rubbers, W is the only function of the first and the second principal invariants of B [Ogden, 2003].

$$\sigma = 2 \left(\frac{\partial W}{\partial I_1} B + \frac{\partial W}{\partial I_2} (I_1 B - B^2) \right) - pI \quad (2.11)$$

where I is the identity tensor, and p is the hydrostatic pressure, determined from boundary conditions. In this study, the Neo-Hookean constitutive model's energy density function was initially assumed [Ogden, 2003], where CI is a material parameter that is obtained from the results of the tensile test. In this test, the material was stretched in one direction ($\sigma_z = \sigma$) while it remained stress-free in all other directions ($\sigma_x = \sigma_y = 0$). For uniaxial loading conditions, the nonzero Cauchy stress component is:

$$\sigma_z = 2C_1 \left(\lambda^2 - \frac{1}{\lambda} \right) = 2C_1 \left(\frac{3\varepsilon_z + 3\varepsilon_z^2 + \varepsilon_z^3}{1 + \varepsilon_z} \right), \quad \lambda = 1 + \varepsilon_z \quad (2.12)$$

Then, in Eq. (2.8), to obtain the energy absorption of the failure of primary yarns, stress elastic (linear) materials, and stress hyperelastic (nonlinear) materials from relation (2.9) and relation (2.12), respectively were used.

2.1.4. Energy absorption of the deformation of secondary yarns (Region 2) under projectile pressure

The region surrounding the impacted zone up to which the transverse stress wave travels along the in-plane directions is referred to as Region 2 (Fig. 1). The layers in Region 2 also experience transverse strain along the thickness direction. Thus, the general energy absorbed equation due to projectile pressure in Region 1 is as follows:

$$E_{sy,i} = \sum_{i=1}^{i=n} \int_{0.5d_p}^{r_{i,i}} \left(\sum_{i=0}^{i=n-1} \int_{\varepsilon_{zi}^* = i\varepsilon_0 b^{\frac{x}{a}}}^{\varepsilon_{z(i+1)} = (i+1)\varepsilon_0 b^{\frac{x}{a}}} \sigma_z(\varepsilon) d\varepsilon \right) h_1 \{2\pi x - 4d_p\} dx \quad (2.13)$$

where ε_0 is the limit of ultimate strain. In Eq. (2.13), to obtain the energy absorption of the failure of the primary yarns under projectile pressure, stress for elastic (linear) materials, and stress for hyperelastic (nonlinear) materials from relation (2.9) and relation (2.12), respectively were also used.

2.1.5. Energy absorption of delamination and matrix cracking

The portion of the layer composite interface endured delamination and matrix cracking through the matrix may not have cracked completely. This phenomenon resulted from the ballistic impact. The matrix still adhered to the fibers and was not entirely detached from the reinforcement. The tensile strain differed from a maximum rate at the impact point to zero at the point to which the in-plane tensile stress wave had extended. When the strain exceeded the damage threshold strain, the matrix failed in the region around the impact point. Then the matrix cracked, leading to delamination in Mode II. [Naik, 2016]. Therefore the individual energies absorbed by delamination and matrix cracking at the end of time interval after impact were:

$$E_{Mc,i} = \sum_{i=1}^{i=n} P_m \pi A_{ql} h V_m r_{Dl,i}^2 E_m, \quad P_m = 1 - \left(\frac{A_{Mc}}{A_{Target}} \times 100 \right) \quad (2.14)$$

$$E_{Dl,i} = \sum_{i=1}^{i=n} P_d \pi A_{ql} r_{Dl,i}^2 G_{Icd}, \quad P_d = 1 - \left(\frac{A_{Dl}}{A_{Target}} \times 100 \right) \quad (2.15)$$

The factors P_m and P_d are the percentage matrix cracking and the percentage of delamination. A_{Target} is the total area of the target before impact. A_{Mc} and A_{Dl} are the damaged areas after impact. A_{ql} and $r_{Dl,i}$ are the percentage of the corresponding circular area and the damage radius, E_m is energy absorbed by matrix cracking per unit volume, and G_{Icd} is the threshold energy before delamination until the i th time interval or critical dynamic strain energy release rate in mode II. All parameters required for the [Eqs. (2.14) and (2.15)] are measured after the impact and when the composite deformed.

2.1.6. Energy absorption of shear plugging

In the first layers composite, shear plugging absorbed some energy, which caused a sharp decline in the kinetic energy of the projectile and the whole force of the contact. During the first time interval, the forces applied to the projectile were inertial and compressive. The inertial force was estimated by equating the effect in the target of the inertial force reaction to change in the displaced material kinetic energy.

The inertial force is assumed by [Awerbuch and Bodner, 1974]:

$$F_1 = \frac{1}{2} \rho A_p V_0^2 \quad (2.16)$$

where A_p is cross-sectional area of the projectile.

The compressive force is assumed by:

$$F_2 = \sigma_z A_p \quad (2.17)$$

The whole force of the contact impacting on the target is calculated as follows:

$$F_T = F_1 + F_2 \quad (2.18)$$

In the first case of impact, as the projectile penetrates, the energy required to break the yarns by shear plugging is greater than the projectile kinetic energy, which causes the shear plugging of the layers to stop. The number of layers composite that fail by shear plugging depends on the material properties of the target, the laminate

diameter, and the laminate thickness. The energy absorption of shear plugging by the end of i th time interval is given by:

$$E_{Sp,i} = \sum_{i=0}^{i=n} \pi d_p h_1 S_{Sp} h_{1,i} \quad (2.19)$$

where $S_{Sp} = F_T / \pi d_p h_1$ indicates the shear plugging strength.

2.1.7. Process of the proposed theory

Fig. 4 shows the computational presentation process of the proposed theory, demonstrating the structure of the analytical model and its results. It should be noted that briefly implementing the flowchart of the analytical model yields a more detailed view of the research questions that the current paper seeks to answer.

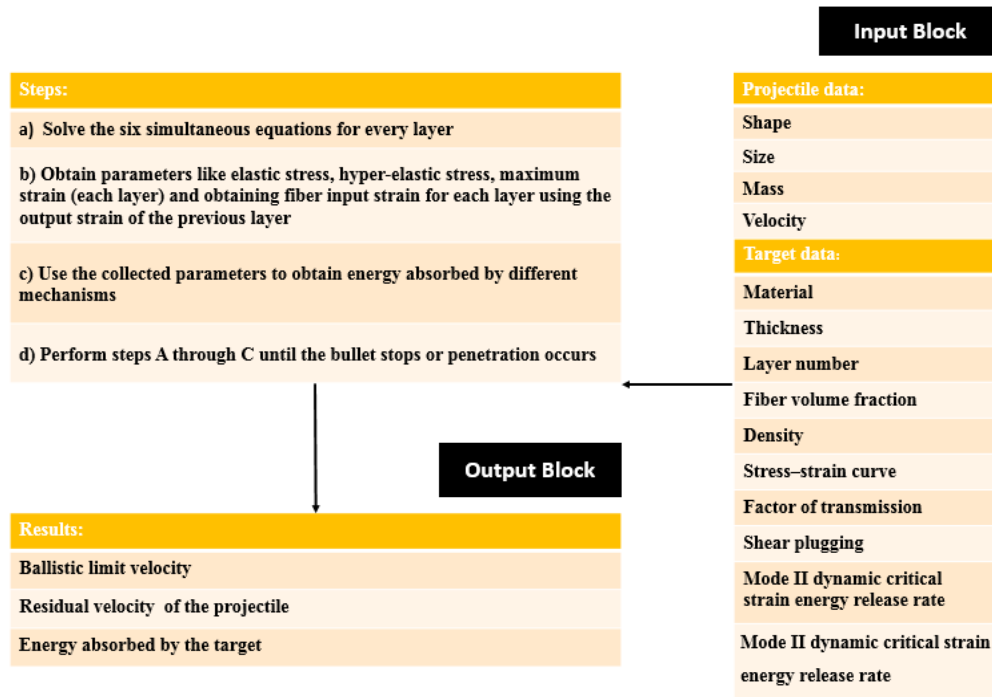


Fig. 4. Flowchart for the analytical model.

3. Model verification

3.1. Materials and Construction

3.1.1. Rubber matrix composite

The fabric and the matrix used in the tensile test were kevlar fabric and natural rubber. To make the natural rubber matrix the vulcanization process was used. This is a chemical method where by a raw natural rubber can be changed into a substance with the desired properties by adding fillers, activators, and sulfur. These additives alter the rubber by creating cross-links between polymer chains. In this study, the HH type of rubber

was used on the shear resistance of rubber matrix composites. The NR compound formulation for the HH type of rubber compound is presented in Table 1. In this study, the HH type of rubber compounding was carried out in an open two-roll mixing mill (Polymix 200 L, Germany) at 40 rpm and the mixing time was 15 min. An Oscillating Disc Rheometer (ODR) model 4308 (Zwick Co., Germany) at 160 °C determined the vulcanization characteristics of the NR compounds. The disc was embedded in the test piece and oscillated through a small specified rotary amplitude to characterize the cure characteristics of the rubber compound [Khodadadi et al., 2019]. The cure characteristics of the rubber compound are presented in Table 2. In this table, t_i indicates the time required for $i\%$ of the torque to increase. The areal density and thickness of the fabric used in the high-velocity impact tests were, respectively, 180 g/m² and 0.23 mm

Table 1. Formulation of compounds [Khodadadi et al., 2019].

Ingredients	Loading (Phr)	
	Company	High Hardness
NR (SMR 20)	The Rubber Research Institute, Malaysia	100
Carbon Black (N330)	Pars, Iran	60
Zink oxide	LG, Korea	5
Calcium carbonate	Yazd Tire, Iran	30
Spindle oil	-	15
Sulfur	LG, Korea	2
Volcacit	-	0.7

Table 2. Curing characteristics [Khodadadi et al., 2019].

	t_5 (min)	t_{10} (min)	t_{90} (min)	t_{95} (min)	t_{100} (min)	The lowest torque on the vulcanization proces M_{max} (kg.cm)	The highest torque on the vulcanization proces M_{max} (kg.cm)
HH rubber	0.28	0.721	2.9	3.4	5.301	8.49	117.28

The impregnation of kevlar fabric for preparing the rubber matrix composite target was facilitated by diluting rubber compound in toluene at a 2:3 vol ratio. Individual fabric layers were soaked in the diluted rubber compound for 24 h. After impregnation with the toluene/rubber mixture, the fabric layers were left in an ambient temperature for 24 h and then put into an oven at 40 °C for 2 h to remove the toluene. Then 2- and 4-coated fabric layers were assembled and subsequently cured under hydraulic pressure at 160 °C by a 25-ton hydraulic press based on rheometer results [Khodadadi et al., 2019].

3.1.2. Thermoset matrix composite

The areal density and thickness of the fabric used in the high-velocity impact tests were, respectively, 180 g/m² and 0.23 mm. The hand lay-up method used TS matrix composite plates to manufacture an epoxy matrix based on ML-506 resin and HA-11 hardener. In this study, the hardness/resin weight ratio of 1/12 was chosen. For the curing process, laminates were kept at constant pressure (15 MPa) for 24 h. The chemical reactions and curing process were carried out at an ambient temperature [Khodadadi et al., 2019].

3.2. Input parameters necessary for the analytical model

To validate the analytical model, the results were compared with the experimental observations from Ref. [Khodadadi et al., 2019]. The behaviours during the ballistic impact of a spherically-ended cylindrical projectile on a kevlar/elastomer and a kevlar/epoxy composite of various thicknesses (1 and 2 mm) were compared. These behaviours were noted in the analytical model described in the preceding section. The ballistic limit, the residual velocity of the projectile, and the cone-shaped surface radius are specified. The input parameters of the model, such as the mechanical properties of the kevlar/elastomer composite target, achieved from the stress-strain curve (Fig. 5(a)) [Khodadadi et al., 2019], and the mechanical properties of the kevlar/epoxy composite target, were derived from the stress-strain curve (Fig. 5(b)) by experimental tests. Necessary tests for the kevlar/epoxy composite samples were conducted according to the Standard Test Method ISO 37:2011(E) in the dumb-bell-shaped type 2 with an effective area of $4 \times 2 \text{ mm}^2$. For each property, three specimens were tested. The experimental tests were carried out to determine the mechanical properties of the reinforced composites at the Impact Engineering General Laboratory of the School of Mechanical Engineering of the Tarbiat Modares University. The mechanical properties of the kevlar/elastomer and kevlar/epoxy composites in the present work are shown in Table 3, respectively. Tensile tests were performed at 0° direction for both kevlar/elastomer [Khodadadi et al., 2019] and kevlar/epoxy composite laminates. The projectile energy was transmitted to the target composite during the incident ballistic impact. During the incident of ballistic impact the energy of the cone's movement was substantial. It should be noted that this was a transient phase. To demonstrate this effect, the total absorbed energy in all figures was eventually, achieved with and without the moving cone energy (E_{KE}).

The projectile and the target specifications for the terms of the analytical model are assumed, such as experimental reference examples [Khodadadi et al., 2019] as follows:

Projectile: a spherically-ended cylindrical, hardened steel projectile with mass, $m_p=9.32 \text{ gr}$; diameter, $d_p=10 \text{ mm}$.

Target: fabric kevlar/elastomer and fabric kevlar/epoxy composites; thickness, $h=1$ and 2 mm ; all samples were fully clamped in a fixture having a $100 \times 100 \text{ mm}^2$ opening.

Fig. 6. shows the boundary conditions of the composite and gas gun device.

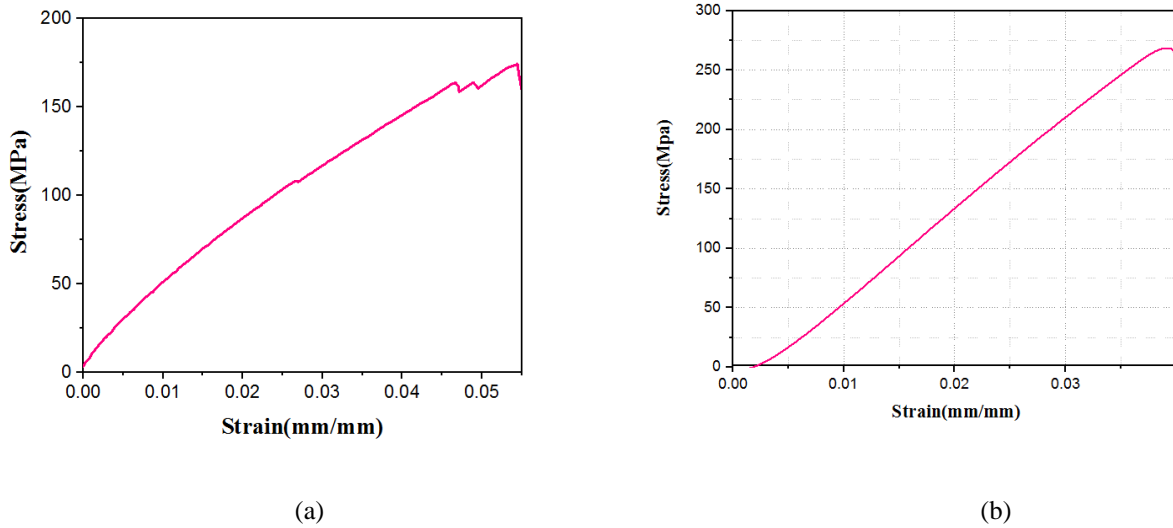


Fig. 5. Tensile stress-strain plot for: (a) fabric kevlar/elastomer composite [Khodadadi et al., 2019] and (b) fabric kevlar/epoxy composite.

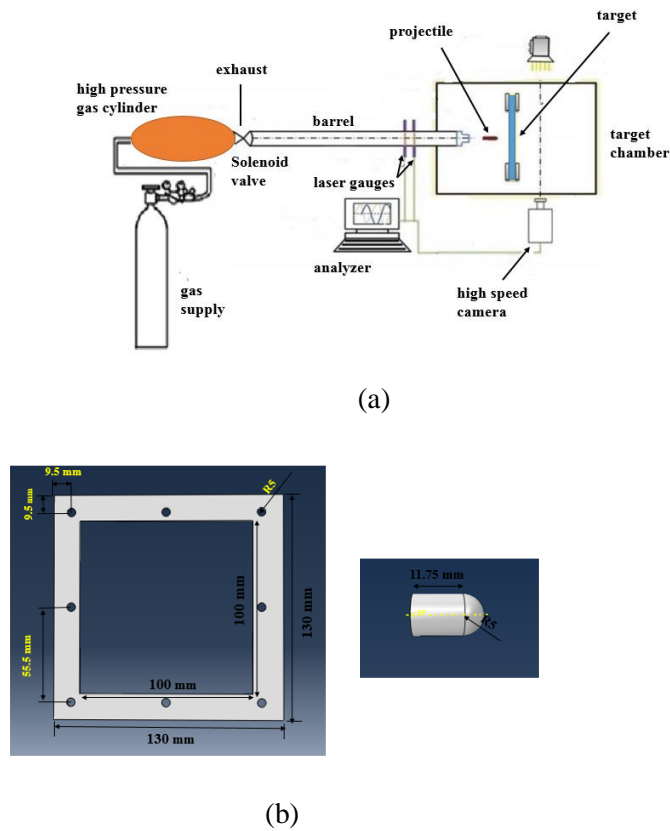


Fig. 6. Schematic of the: (a) gas gun device and (b) fixture used for ballistic tests and technical drawing of projectile.

Table 3. Input parameters required for the analytical predictions of ballistic impact behavior at 0° direction for both kevlar/elastomer and kevlar/epoxy composite laminates.

Projectile details	
Mass (gr)	9.32
Shape	Spherically-ended cylinder
Diameter (mm)	10
Target details [Khodadadi et al., 2019]	

Material	kevlar/elastomer
fiber volume fraction (%)	46
matrix volume fraction (%)	54
Fiber thickness (mm)	0.23
Matrix thickness (mm)	0.27
Layer thickness (mm)	0.5
No. of layers composite	2 / 4
Density (kg/m ³)	1175.4
Tensile failure strain (%)	5.5
Material constant C ₁ (MPa)	0.99
Tensile stress-strain curve	Fig. 5
Quasi-lemniscate area reduction factor	0.4
Stress wave transmission factor	0.85
Delamination percent (%)	40
Matrix crack percent (%)	40
Mode II dynamic critical strain energy release rate (J/m ²)	3850
Matrix cracking energy (MJ/m ³)	-
Shear plugging strength, S _{sp} (GPa)	0.8
<hr/>	
Target details	
Material	kevlar/Epoxy
fiber volume fraction (%)	46
matrix volume fraction (%)	54
Fiber thickness (mm)	0.23
Matrix thickness (mm)	0.27
Layer thickness (mm)	0.5
No. of layers composite	2 / 4
Density (kg/m ³)	1230
Tensile failure strain (%)	3.95
Young's modulus (GPa)	3.520
Quasi-lemniscate area reduction factor	0.9
Stress wave transmission factor	0.85
Delamination percent (%)	90
Matrix crack percent (%)	90
Mode II dynamic critical strain energy release rate (J/m ²)	2485
shear plugging (MPa)	9
Matrix cracking energy (MJ/m ³)	0.9

3.3. Comparison of the ballistic limit velocity

The ballistic limit velocity using the analytical model is predicted for various target thicknesses (see Tables 4 and 5). The ballistic limit for the fabric kevlar/elastomer composite of two and four layers according to Table 4 was obtained; it was respectively, 66.06 m/s and 107.2 m/s. Corresponding to the analytical model presented, the ballistic limit for the fabric kevlar/epoxy composite of two and four layers according to Table 5, was respectively, 26.73 m/s and 39.03 m/s.

The ballistic limit achieved from the analytically predicted model was compared with the experimental observations for fabric kevlar/elastomer and kevlar/epoxy composites [Khodadadi et al., 2019]. As shown in Tables 4 and 5, the percentage difference between the ballistic limit results for 2- and 4-layer kevlar/elastomer composites are, respectively, 10% and 2.4%. Also, this percentage difference is respectively 2.8% and 5.9%

for 2- and 4-layer kevlar/epoxy composites. Therefore, there is a good agreement between the analytical model and the experimental observations [Khodadadi et al., 2019].

Table 4 - Ballistic impact results for the kevlar/elastomer composite.

Projectile mass, m_p (gr)	Projectile diameter, d_p (mm)	Target thickness, h(mm)	Predicted damage size, r_{del} (mm)	Predicted surface radius of the cone, r_t (mm)	Predicted V_b (m/s)	Exp. V_{50} (m/s) [Khodadadi et al., 2019]	Difference (%)
9.32	10	1	4.7	10	66.06	68	2.8
9.32	10	2	6.8	9	107.27	114	5.9

Table 5 - Ballistic impact results for the kevlar/epoxy composite.

Projectile mass, m_p (gr)	Projectile diameter, d_p (mm)	Target thickness, h(mm)	Predicted damage size, r_{del} (mm)	Predicted surface radius of the cone, r_t (mm)	Predicted V_b (m/s)	Exp. V_{50} (m/s) [Khodadadi et al., 2019]	Difference (%)
9.32	10	1	2.1	7.75	26.73	30	10
9.32	10	2	2.85	12	39.03	40	2.4

3.4. Comparison of the energy absorption

Fig. 7 presents the results for the kevlar/elastomer composite of two and four layers. The contribution of each mechanism to the energy absorption process at various velocities can be observed. These results indicate the high-velocity penetration. In this case, with the energy absorption of different mechanisms ($V_i=113$ m/s in the 2-layer composite) the kinetic energy of the projectile is 31.67 J.

The highest absorbed energies are as follows. The energy absorbed in plugging the layers is 39.65%, the absorbed energy of the primary yarns is 35.55%, the absorbed energy of the secondary yarns is 15.59%, the absorbed energy of the moving cone is 8.9%; the energy absorption of the delamination between the layers is 0.30 %, and the energy absorbed by matrix cracking is 0%. In the other case, with the energy absorption of different mechanisms ($V_i=145$ m/s in the 4-layer composite), the kinetic energy of the projectile is 72.45 J. The mechanisms that have the highest energy absorption are, in turn, the energy absorbed by primary yarns is 50.18%; the energy disintegrated by plugging of the layers is 34.68%; the energy absorbed by secondary yarns is 10.7%; the energy absorption of the moving cone is 4.27%; the energy absorption of the delamination between the layers is 0.16%, and the energy absorbed by matrix cracking is 0%.

The results are presented in Fig. 8 for the kevlar/epoxy composites of two and four layers. The contribution of each mechanism to the energy absorption process at various velocities can be observed. These results were recorded at high-velocity penetration. In this case, the energy absorption of various mechanisms ($V_i=111$ m/s in

the two-layer composite), the incident kinetic energy of the projectile is 6.76 J. The mechanisms that received the most significant energy absorption are as follows. The energy dissipated by the kinetic energy of the moving cone is 46.59%; the energy absorption of the primary yarns is 39.20%; the energy absorption of secondary yarns is 7.98%; the energy absorption of the delamination between the layers is 3.55 %; the energy absorption of plugging of the layers is 2.07%, and the energy absorbed by matrix cracking is 0.71%.

In the other case, concerning the energy absorption of various mechanisms with $V_i = 117$ m/s in a four-layer composite, the incident projectile kinetic energy is 14.29 J. The most significant absorptions are as follows. The energy absorbed by the primary yarns is 61.58%, the kinetic energy of the moving cone is 29.53 %, the energy absorbed of secondary yarns is 5.73%, the energy absorption of plugging of the layers is 1.95%; the energy absorption of the delamination between the layers is 0.89 %, and the energy absorbed by matrix cracking is 0.34%.

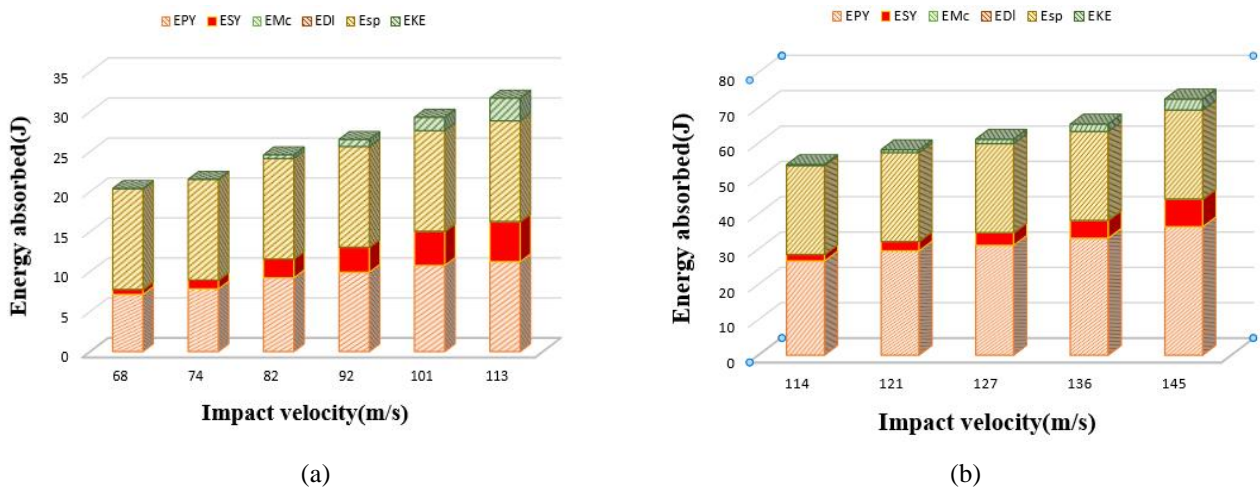


Fig. 7. Comparison of the various mechanisms of energy absorption during a ballistic collision model to deal with various velocities on the kevlar/elastomer composite: (a) with a thickness of 1 mm and (b) with a thickness of 2 mm.

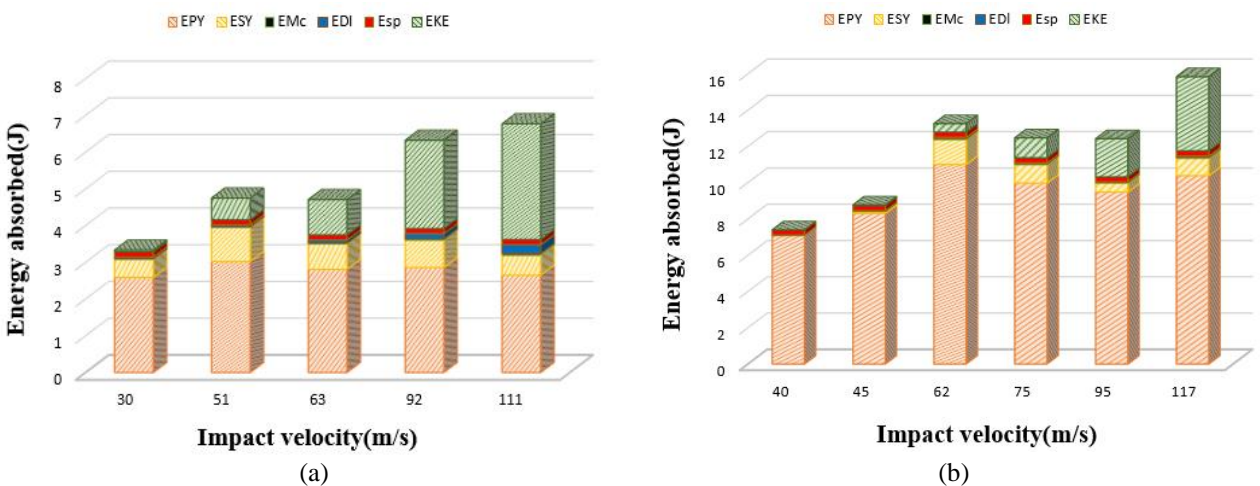


Fig. 8. Comparison of the various mechanisms of energy absorption during a ballistic collision model to deal with various velocities on the kevlar/epoxy composite: (a) with a thickness of 1 mm and (b) with a thickness of 2 mm.

The energy absorption is predicted for various velocities when the impact is on the kevlar/elastomer composite and the kevlar/epoxy composite with multi thicknesses, and the energy absorption between the analytical and experimental results may be compared [Khodadadi et al., 2019]. A velocity penetration model is presented in Figs. 9 and 10. It can be found that the agreement between the analytical model and experimental results is good.

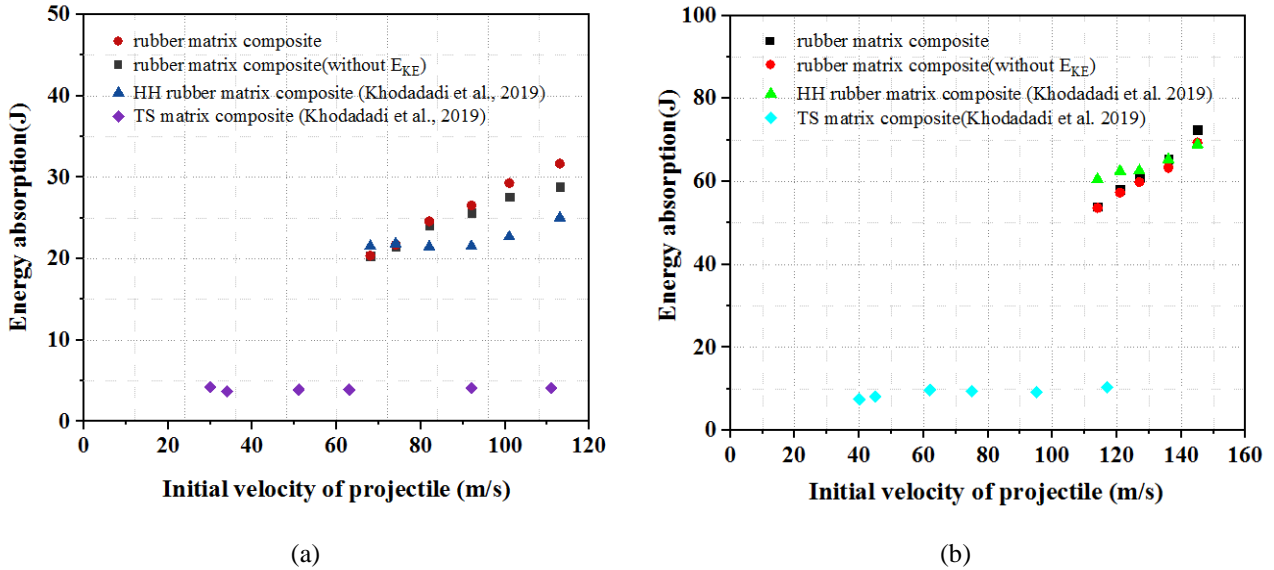


Fig. 9. Comparison of energy absorption between analytical and experimental model during a ballistic collision with various velocities on the target layer kevlar/elastomer composite: (a) with a thickness of 1 mm and (b) with a thickness of 2 mm.

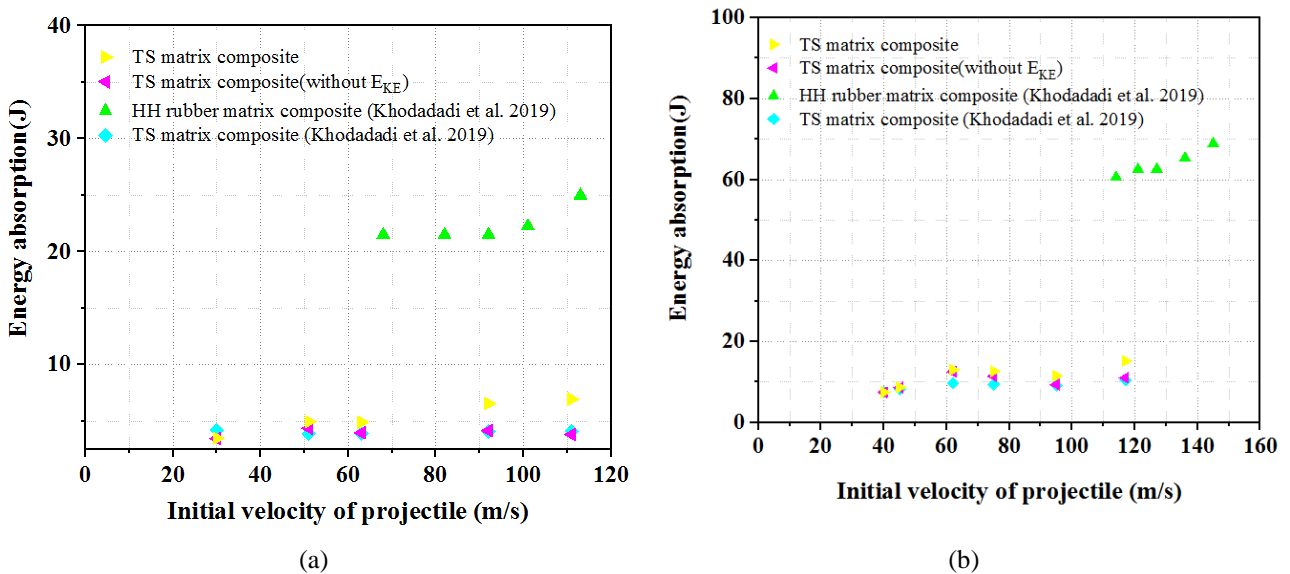


Fig. 10. Comparison of the various mechanisms of energy absorption during a ballistic collision model to deal with various velocities on the kevlar/epoxy composite: (a) with a thickness of 1 mm and (b) with a thickness of 2 mm.

Moreover, to compare Figs. 9 and 10, at the same initial velocities of the projectile, the energy absorption of the elastomeric composite is higher than the thermoset composite. This emerges as the crucial role of an elastomer matrix; it increases the energy absorption of the composite. For example, the energy absorption for a 2-layer kevlar/elastomer composite with an initial velocity of 92 m/s is 26.53 J; however, the energy absorption

for a 2-layer kevlar/epoxy composite at the same initial velocity is 6.32 J. These results are also valid for the 4-layer composites.

The energy absorbed at various velocities for the kevlar/elastomer 2- and 4-layer composite and the kevlar/epoxy 2- and 4-layer composite is shown in Tables 6 to 9. By comparing the absorbed energy obtained from the analytical model presented in these tables, it can be found that the absorbed energy increases with the increase in the velocity of the impact. Thicker laminates also absorb more energy than thin laminates. Furthermore, the effect of the energy is mainly achieved by the moving cone during the ballistic impact. This may indicate that this is a transient phase.

In addition, at higher ballistic velocities, due to the increase in velocity, the difference between the initial energy of the projectile and the absorbed energy increases with a steep slope [Naik and Shrirao, 2004], and the absorbed energy will be a small fraction of the impact energy. Therefore, it shows that the accuracy of the calculated output speed can not indicate the accuracy of the proposed theory. As a result of comparing the results of the analytical model presented with the experimental results of other researchers, the most errors are encountered.

As can be seen, the average error of absorbed energy of the kevlar/elastomer 2- and 4-layer composites with the energy of the moving cone (E_{KE}) is respectively 16.57% and 5.14%, and without the energy of the moving cone (E_{KE}) is respectively 12.59% and 5.55%. In addition, the average error of absorbed energy of the kevlar/epoxy 2- and 4-layer composites with the energy of the moving cone (E_{KE}) is respectively 25% and 18.82%, and without the energy of the moving cone (E_{KE}) is respectively 12.45% and 5.53%. The average error of absorbed energy of the Kevlar/epoxy 2- and 4-layer composites with the energy of the moving cone is bigger than that of without the energy of the moving cone. In comparison, these results for the Kevlar/ elastomer 2- and 4-layer composites is less. It can be found that the contribution of the energy absorption of the moving cone for the Kevlar/epoxy 2- and 4-layer composites is higher than the Kevlar/ elastomer 2- and 4-layer composites according to Figs. 7 and 8.

The model's accuracy in predicting the absorbed energy shows that, with an increase of the kevlar/elastomer composite layers, it is more useful to consider the energy absorbed by the formed cone because it reduces more of the average percentage of error of the analytical model above that of the experimental results. However, increasing the kevlar/epoxy composite layers is not an efficient solution, given the energy absorbed by the formed cone, and it increases the average percentage of error of the analytical model above that of the experimental results.

Hence, it appears that the error is very clearly permissible. Generally, there is a decent match between the analytical model and experimental results [Khodadadi et al., 2019].

Table 6. Comparing the amount of energy absorbed during ballistic impact with various velocities on the kevlar/elastomer composite with a thickness of 1 mm.

The initial velocity (m/s)	Predicted Surface radius (mm)of the cone, r_t	Predicted Damage size, r_{del} (mm)	Exp. energy absorbed (J) [Khodadadi et al., 2019]	Predicted energy absorbed (J)	Difference (%)	Predicted energy absorbed (without E_{KE}). (J)	Difference (%)
68	10	4.7	21.54	20.38	5.38	20.34	5.57
74	11	5	21.86	21.7	0.73	21.52	1.57
82	13	5.4	21.47	24.59	14.53	24.14	12.43
92	14	5.9	21.53	26.53	23.22	25.63	19.04
101	15.25	6.35	22.70	29.30	29.07	27.63	21.71
113	16	6.95	25.03	31.67	26.52	28.85	15.26

Table 7. Comparing the amount of energy absorbed during ballistic impact with various velocities on the kevlar/elastomer composite with a thickness of 2 mm.

The initial velocity (m/s)	Predicted Surface radius (mm)of the cone, r_t	Predicted damage size, r_{del} (mm)	Exp. energy absorbed (J) [Khodadadi et al., 2019]	Predicted energy absorbed (J)	Difference (%)	Predicted energy absorbed (without E_{KE}). (J)	Difference (%)
114	9	6.8	60.56	53.90	10.99	53.63	11.44
121	10	7.05	62.51	58.11	7.03	57.31	8.31
127	10.55	7.25	62.56	61.09	2.34	59.85	4.33
136	11.25	7.55	65.27	65.38	0.17	63.30	3.01
145	12.40	7.85	68.9	72.45	5.16	69.35	0.65

Table 8. Comparing the amount of energy absorbed during ballistic impact with various velocities on the kevlar/epoxy composite with a thickness of 1 mm.

The initial velocity (m/s)	Predicted Surface radius (mm)of the cone, r_t	Predicted damage size, r_{del} (mm)	Exp. energy absorbed (J) [Khodadadi et al., 2019]	Predicted energy absorbed (J)	Difference (%)	Predicted energy absorbed (without E_{KE}). (J)	Difference (%)
30	12	2.85	4.2	3.33	2.07	3.28	21.90
51	14	3	4.29	4.75	10.72	4.16	3.03
63	13	3.75	3.9	4.7	20.51	3.74	4.10
92	13.25	5	4.98	6.32	26.90	3.92	21.28
111	12.25	6.25	4.1	6.76	64.8	3.61	11.95

Table 9. Comparing the amount of energy absorbed during ballistic impact with various velocities on the kevlar/epoxy composite with a thickness of 2 mm.

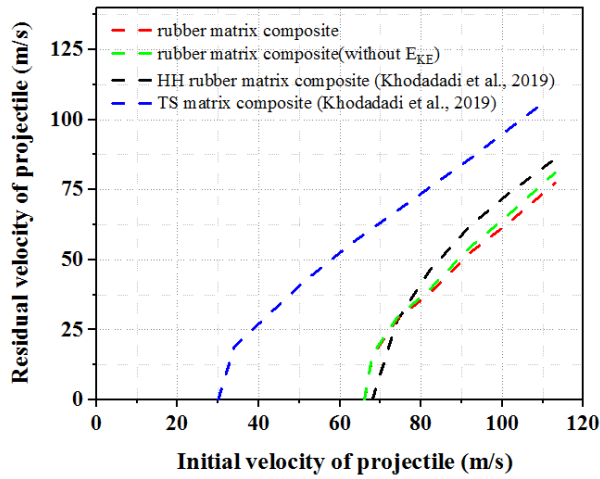
The initial velocity (m/s)	Predicted Surface radius (mm)of the cone, r_t	Predicted damage size, r_{del} (mm)	Exp. energy absorbed (J) [Khodadadi et al., 2019]	Predicted energy absorbed (J)	Difference (%)	Predicted energy absorbed (without E_{KE}). (J)	Difference (%)
----------------------------	---	---------------------------------------	---	-------------------------------	----------------	--	----------------

40	7.75	2.1	7.45	7.10	4.69	7.09	4.83
45	8.35	2.85	8.24	7.88	4.36	7.79	5.46
62	11	4.55	10.46	12.02	14.91	11.43	9.27
75	10.35	3.85	9.99	11.67	16.81	10.38	3.90
95	9.25	3.4	9.17	11.08	20.82	8.89	3.05
117	10.15	4.5	9.44	14.29	51.37	10.07	6.67

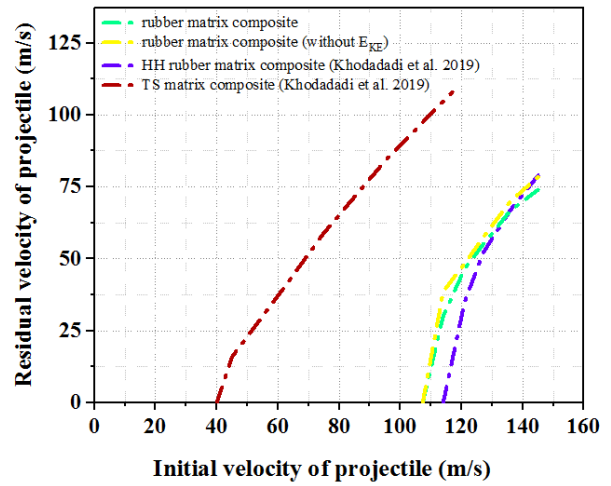
3.5. Comparison of residual velocity

A function of the velocity of the event of ballistic impact can be shown as the residual velocity of projectile (V_r) in Figs. 11 and 12. These figures are for the case where $h = 1$ and $h = 2$, $m_p = 9.32\text{g}$, $d_p = 10\text{mm}$. The results show that the residual velocities of a projectile for a 2-layer kevlar/elastomer composite with initial velocities of 74 m/s and 113 m/s are, respectively, 61.34% and 31.61% lower than their initial collision velocity. In comparison, these results for a 2-layer kevlar/epoxy composite with initial velocities of 51 m/s and 111 m/s are, respectively, 22.07% and 6.08%. The results for the residual velocities of a projectile of 4-layer kevlar/elastomer composite with initial velocities of 121 m/s and 145 m/s are 61.49% and 48.97 % lower than their initial velocities on impact. However, the residual velocities of a projectile for a 4-layer kevlar/epoxy composite with initial velocities of 45 m/s and 117 m/s are 59.35% and 11.92 % lower than their initial collision velocities.

In the residual velocity of the projectile plot against the incident velocity of ballistic impact, it can be accurately seen that when the velocity of the incident ballistic impact increases above the ballistic limit velocity, the residual velocity is similarly increased. However, this increase for 2- and 4-layer kevlar/elastomer composites has a higher slope just above the ballistic limit than the 2- and 4-layer kevlar/epoxy composites. In this instance, the kevlar/elastomer 2-layer composite is not perforated at all at a ballistic impact velocity of 66.06 m/s. However, when the velocity of the ballistic impact is 68 m/s, perforation does occur at the residual velocity of 15.78 m/s and the kevlar/epoxy composite of 2-layer is not perforated when the ballistic impact is 26.73 m/s. Nevertheless, when the velocity of the ballistic impact is 30 m/s, the composite is perforated at the residual velocity of 13.60 m/s. This can be explained by the projectile movement and the increase of the surface radius cone during the ballistic impact. In the event of a ballistic impact, the higher layers will be discrete, while the lower layers may not be discrete. At first, the strain increases and then begins to decrease in the lower layers. It will depend on the geometry of the cone determined at any time by a change in the height and surface radius of the cone. If the tensile strain has previously exceeded what is permissible, as soon as it makes a perforation it declines. Then the cone geometry is formed. However, the strain imposed by the projectile displacement (the change in cone height (h_i) and the transverse cone radius (r_i)) can be determined at any time.

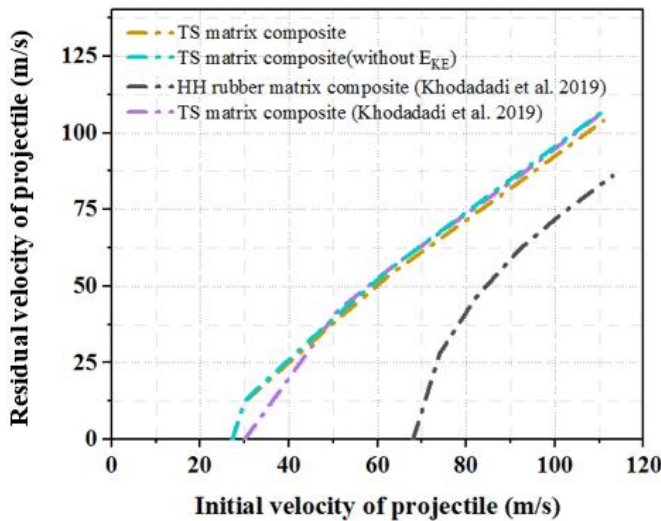


(a)

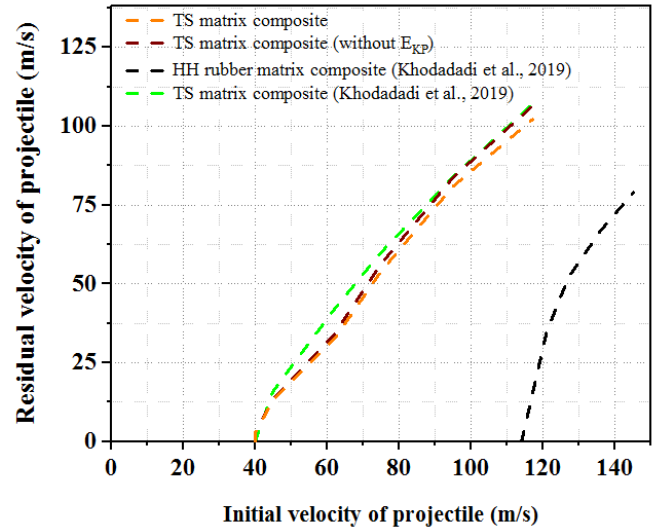


(b)

Fig. 11. Comparison of the residual analytical and experimental velocities on the target layer kevlar/elastomer composite: (a) with a thickness of 1 mm and (b) with a thickness of 2 mm.



(a)



(b)

Fig. 12. Comparison of residual analytical and experimental velocities on the target layer kevlar/epoxy composite: (a) with a thickness of 1 mm and (b) with a thickness of 2 mm.

In addition, to compare Figs. 11 and 12, at the same initial velocity of the projectile, the residual velocities of the thermoset composite are higher than those of the elastomeric composite. For example, the residual velocities for a 2-layer kevlar/elastomer and a 2-layer kevlar/epoxy composite with an initial velocity of 92 m/s are, respectively, 52.44 m/s and 84.29 m/s. It will be seen that the elastomer matrix is more useful for reducing the residual velocities of the composite than the epoxy matrix. This result is also applicable to a 4-layer kevlar/elastomer and a 4-layer kevlar/epoxy composite.

3.6. Study on the effect of the target's thickness

The target thickness effect on the impact and the projectile residual velocities are plotted in Fig. 13, comparing the impact resistance of the kevlar/elastomer laminate with the kevlar/epoxy laminate with thicknesses of 1 mm

and 2 mm. By increasing the incident ballistic impact velocity for the same diameter and mass of the projectile, the residual velocity also increases. The lowest ballistic limit velocity of the projectiles is detected for impact on a 1 mm thick composite. For example, regarding the impact on a 2 mm thick composite laminate, the ballistic limit velocity is the highest in both composites. Increasing the thickness of the target increases the velocity of the ballistic limit. However, as the thickness of the target increases, the rate of increase in the ballistic limit velocity declines. This also goes for the same velocity of the ballistic limit projectile: increasing the target thickness reduces the residual velocity. Moreover, the residual velocity on the kevlar/elastomer composite at the above thicknesses is less than the residual velocity on the kevlar/epoxy composite. This indicates the high energy absorption of the elastomeric composite compared to the thermoset composite; it caused the fiber in all parts of the composite to affect the ballistic performance due to the presence of the elastomer and its effect on the fiber's flexibility.

In addition, in the lower initial velocities close to the ballistic limit, the curves (with E_{KE} and without E_{KE}) are almost the same, and the cone-formation on the back face of the target is less common because the composite cannot withstand projectile exit [Morye et al., 2000]. But with increasing the initial velocities much higher than the ballistic limit, the composite target prevents the projectile from leaving. The cone-formation on the back face of the target after impact is different in that it depends on the material of the composite matrix.

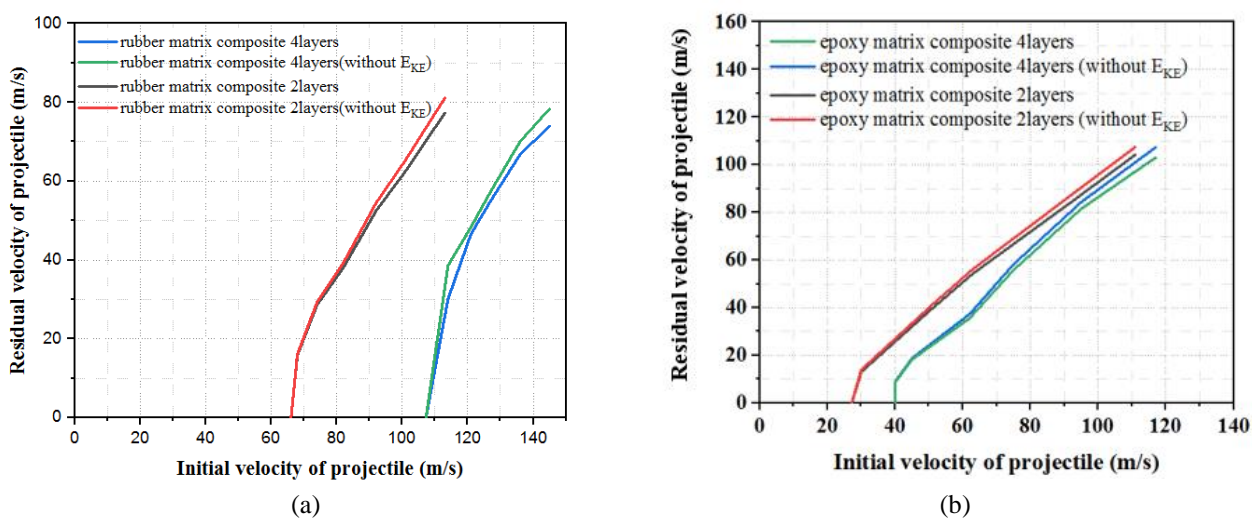


Fig. 13. Comparison of residual velocities curve: (a) between the 2- and 4-layer kevlar/elastomer composites at the velocity of the ballistic limit and (b) between the 2- and 4-layer kevlar/epoxy composites at the velocity of the ballistic limit.

4. The effects of shear on delamination in layer laminates

The separation of fiber and matrix in the composite can be studied to calculate the amount of shear stress and shear strain. The rotation of the composite test samples can cause damage in the fiber and matrix such as debonding, delamination, and matrix cracking, which will negatively affect the composite shear strength. For this reason, it is essential to prevent the rotation of the composite samples. Experimental tests were carried out to determine the in-plane shear properties of reinforced composites with different matrices at the Polymer Engineering General Laboratory of the School of Chemical Engineering of the Tarbiat Modares University.

Experiments using the tensile testing of at $\pm 45^\circ$ laminates at a test speed of 500 mm/min. According to the Standard Test Method ISO 37:2011(E), samples in dumb-bell-shaped type 2 with an effective area of $4 \times 2 \text{ mm}^2$ were provided and cut using the water jet cutting method (Fig. 14).

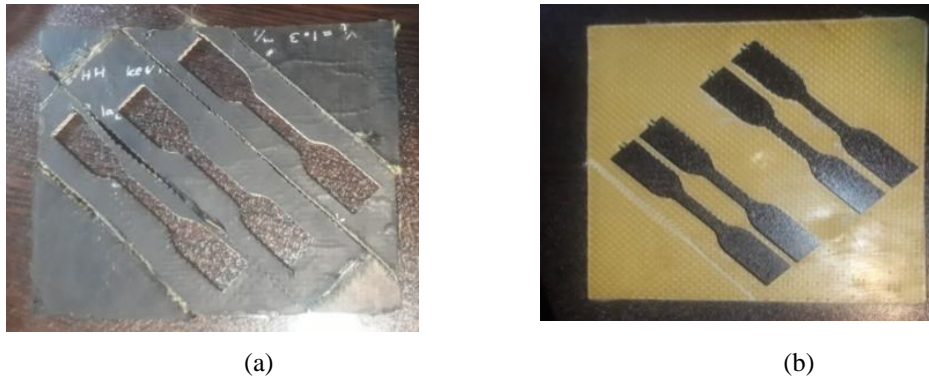


Fig. 14. Samples cut at $\pm 45^\circ$ laminates from: (a) composite kevlar/elastomer and (b) composite kevlar/epoxy.

According to ISO 37: 2011 (E), the in-plane shear stress of the samples was derived from the following equation:

$$\tau_{Shear} = \frac{P_{Load}}{2A} \quad (4.1)$$

The factors P_{Load} , A and τ_{Shear} indicate the applied load, cross-section (effective area), and in-plane shear stress. Fig. 15 shows the in-plane shear stress of different composites.

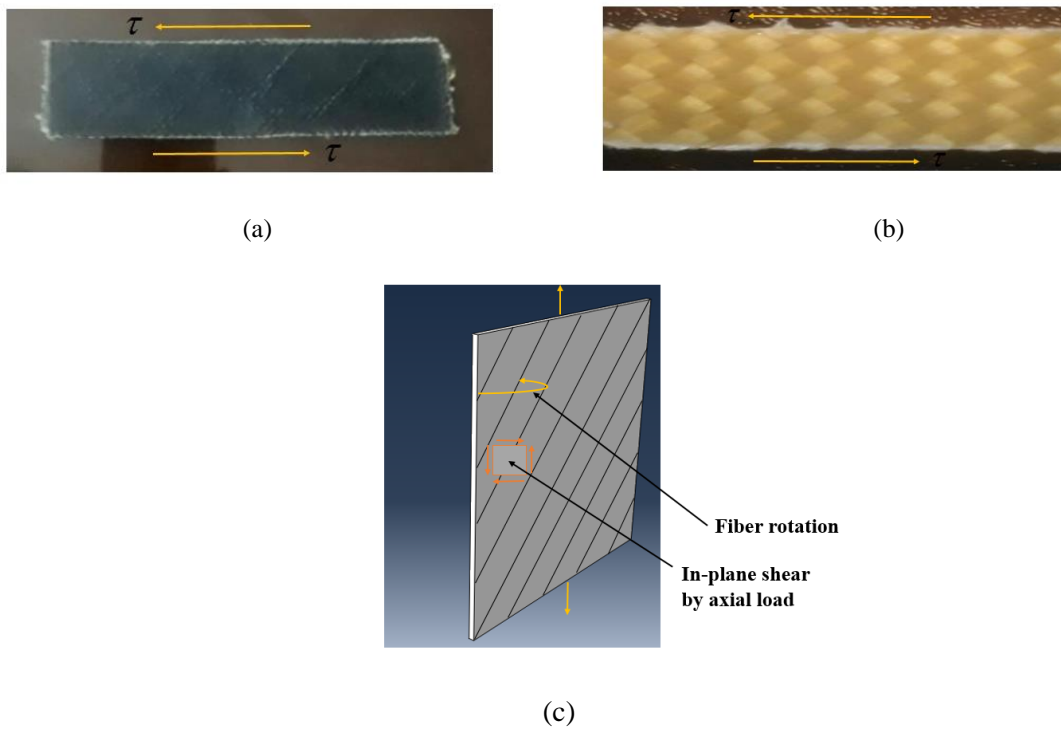


Fig. 15. (a) The shear stress of kevlar/elastomer composite, (b) the shear stress of kevlar/epoxy composite and (c) schematic illustration of axial tensile loading of angle layer laminates.

The role of the matrix was to connect the fibers and make available the load transfers between them. The axial fibers withstood most of the load, and the role of the interface was limited. The interface commonly fails under a normal tensile load. However, Fig. 15 is a schematic illustration of how axial tensile loading of angle layer laminates causes rotation of the layers in which $\pm 45^\circ$ laminates causes shear stress at the interface between fiber and matrix. This rotation is one of the essential factors in delamination. In addition, it increases the stress concentration factor of the layers and local instability, which leads to an increase in the growth of delamination, resulting in a compressive failure of the laminate. Hence, delamination is identified as the most widespread life restricting growth destroying mode, which indirectly affects the ultimate failure of the construction and thus its life.

The interface must be strong enough to transfer the shear, and the in-plane shear stress is created to be highly dependent on the matrix at the composite. The matrix material must be flexible enough to take up the large shear deformation. In the previous sections, the energy absorption, tensile strength, and strain failure of elastomeric composites were investigated at 0° direction. But in this section, tensile tests carried out on $\pm 45^\circ$ laminates to assess the shear stress on the lamina and shear strain response of the kevlar/elastomer composite and the kevlar/epoxy composite. These test results also form a computer conditional shear stress and shear strain plot for the fiber coordinates $\pm 45^\circ$, which is presented in Fig. 16 for the kevlar/elastomer composite and the kevlar/epoxy composite. This figure shows that the shear stress of the kevlar/epoxy composite is higher than that of the kevlar/elastomer composite.

It causes greater separation of the thermoset composite layers because shear stress is a factor for delamination. Still, the separation of layers of the elastomeric composite according to the amount of its shear stress is less likely to occur. The elastomer matrix effect on the shear strain is also greater than the epoxy matrix, and the shear strain increases to a maximum of 1.52 times. According to Figs. 7(a) and 8(a) (section 3.4) were obtained the contribution of the energy absorbed by the delamination between the layers with $V_i = 92$ m/s in a two-layer elastomeric composite is 0.067J, and in a two-layer thermoset composite is 0.15J. It can be seen that the adhesion of kevlar fibers by the elastomer is more substantial than by the epoxy resin, which increases the shear strain of the elastomeric composites against failure and reduces the separation between the fibers and the matrix. As well as, it can be concluded that elastomeric composites compared to thermoset composites due to their high flexibility due to the effect of an elastomer matrix in increasing the tensile strength of this type of composites, prevents the separation of layers. Therefore, this makes it possible to use these composites in various industries, especially in heavy impacts.

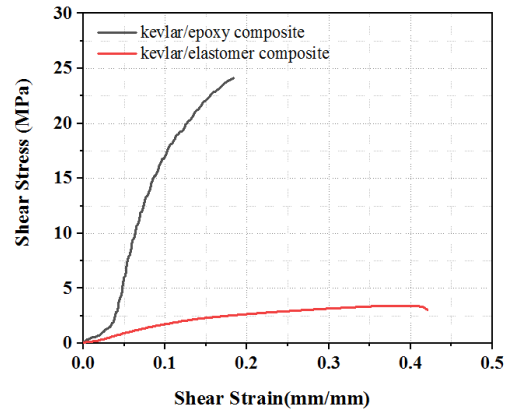


Fig. 16. Shear stress plot for the fiber coordinates $\pm 45^\circ$ for the kevlar/elastomer composite and the kevlar/epoxy composite.

5. Conclusions

This study may be called a comprehensive model; in it, we have sought to design and implement a simple, efficient, and reliable model of important mechanisms for energy absorption which allowed good congruence between the analytically predicted and experimental results. We also wanted a good match between the amounts of energy calculated from the theoretical mechanisms studied in this model and the experimental data. The model's accuracy in this comparison was 10-20%, which is suitable for engineering calculations. In the residual velocity of a projectile plot against the ballistic impact velocity, it can be accurately seen that when the velocity of the event ballistic impact increases above the velocity of the ballistic limit, the residual velocity is correspondingly increased. However, just above the ballistic limit, the increase is very sudden. The significance of energy absorption mechanisms depends on the material, type, and method of the target's construction. The high energy absorption of the kevlar/elastomer composite can be ascribed to the role of the elastomer matrix, which thanks to its high energy absorption properties, and great flexibility. This factor has a more influential role in improving ballistic performance than the kevlar/thermoset composite. Because they cause the fibers inside the impact range and the fibers outside the impact range to affect the ballistic performance and as a result, elastomeric composites absorb more energy. Increasing the composite thickness on the high energy absorption makes the effect of the elastomer noticeable. The rubber matrix, by great flexibility, makes the fabric layers stick together and the layers act more effectively against the projectile.

The amount of shear strain and shear stress in studying the separation of fiber and matrix in the different composites was investigated. The in-plane shear stress is a kind of interaction between other processes that complicates failure prediction in laminates by delaying the beginning of fiber failure. In addition, the role of matrix is to connect the fibers and make available the load transfers between them. The elastomer matrix is used in the present work to increase this load and then have its shear stress/strain compared with that of the epoxy matrix. It can be found that the effect of the elastomer matrix on the in-plane shear was more than the effect of the epoxy matrix, and the percentage increased between the shear strain elastomeric composites compared to thermoset composites is 152%. The calculation results demonstrated that the adhesion of kevlar fibers by elastomer is more substantial than by epoxy resin, which causes an increase in the energy absorption

and the shear strain failure of elastomeric composites against failure, and reduces the separation between the fibers and the matrix.

Acknowledgments

The authors gratefully acknowledge Tarbiat Modares University for providing necessary experimental facilities and technical support.

References

- Ahmadi, H., Sabouri, H., Liaghat, G., and Bidkhor, E. [2011] "Experimental and numerical investigation on the high velocity impact response of GLARE with different thickness ratio," *Procedia Engineering* **10**, 869-874
- Ahmadi, H., and Liaghat, G. [2019] "Analytical and experimental investigation of high velocity impact on foam core sandwich panel," *Polymer Composites* **40**(6), 2258-2272.
- Awerbuch, J., and Bodner, S. [1974] "Experimental investigation of normal perforation of projectiles in metallic plates," *International Journal of Solids and Structures* **10**(6), 685-699.
- Brinson, H. F., and Brinson, L. C. [2008] "Polymer engineering science and viscoelasticity," *An introduction*, pp. 99-157.
- Bresciani, L. M., Manes, A., and Giglio, M. [2015] "An analytical model for ballistic impacts against plain-woven fabrics with a polymeric matrix," *International Journal of Impact Engineering* **78**, 138-149.
- Benzait, Z., and Trabzon, L. [2018] "A review of recent research on materials used in polymer-matrix composites for body armor application," *Journal of Composite Materials* **52**(23), 3241-3263.
- Guoqi, Z., Goldsmith, W., and Dharan, C. H. [1992] "Penetration of laminated Kevlar by projectiles—I. Experimental investigation," *International Journal of Solids and Structures* **29**(4), 399-420.
- Khodadadi, A., Liaghat, G., Bahramian, A. R., Ahmadi, H., Anani, Y., Asemanni, S., and Razmkhah, O. [2019] "High velocity impact behavior of Kevlar/rubber and Kevlar/epoxy composites: A comparative study," *Composite Structures* **216**, 159-167
- Kumar, S., Gupta, D. S., Singh, I., and Sharma, A. [2010], "Behavior of Kevlar/epoxy composite plates under ballistic impact," *Journal of Reinforced Plastics and Composites* **29**(13), 2048-2064.
- Mahesh, V., Joladarashi, S., and Kulkarni, S. M. [2021] "Damage mechanics and energy absorption capabilities of natural fiber reinforced elastomeric based bio composite for sacrificial structural applications," *Defence Technology* **17**(1), 161-176.
- Mamivand, M., and Liaghat, G. [2010] "A model for ballistic impact on multi-layer fabric targets," *International Journal of Impact Engineering* **37**(7), 806-812.
- Meyers, M. A. [1994], *Dynamic behavior of materials*, John Wiley & Sons.
- Morye, S., Hine, P., Duckett, R., Carr, D., and Ward, I. [2000] "Modelling of the energy absorption by polymer composites upon ballistic impact," *Composites science and technology* **60**(14), pp. 2631-2642.
- Naik, N. [2016] "Analysis of woven fabric composites for ballistic protection," *Advanced Fibrous Composite Materials for Ballistic Protection*, pp. 217-262.
- Naik, N., and Doshi, A. [2008] "Ballistic impact behaviour of thick composites: Parametric studies," *Composite structures* **82**(3), 447-464.
- Naik, N., and Shirao, P. [2004] "Composite structures under ballistic impact," *Composite structures* **66**(1-4), 579-590.
- Naik, N., Shirao, P., and Reddy, B. [2006] "Ballistic impact behaviour of woven fabric composites: Formulation," *International journal of impact engineering* **32**(9), 1521-1552.
- Ng, S. S., Li, C., and Chan, V. [2011] "Experimental and numerical determination of cellular traction force on polymeric hydrogels," *Interface focus* **1**(5), 777-791.
- Ogden, R. W. [2003] "Nonlinear elasticity, anisotropy, material stability and residual stresses in soft tissue," *Biomechanics of soft tissue in cardiovascular systems*, pp. 65-108.
- Pandya, K. S., Dharmane, L., Pothnis, J. R., Ravikumar, G., and Naik, N. [2012] "Stress wave attenuation in composites during ballistic impact," *Polymer Testing* **31**(2), 261-266.
- Pol, M. H., Liaghat, G., Zamani, E., and Ordys, A. [2015] "Investigation of the ballistic impact behavior of 2D woven glass/epoxy/nanoclay nanocomposites," *Journal of Composite Materials* **49**(12), 1449-1460.
- Thiruvarudchelvan, S. [1993] "Elastomers in metal forming: a review," *Journal of Materials Processing Technology* **39**(1-2), 55-82.

Tubaldi, E., Mitoulis, S. A., and Ahmadi, H. [2018] "Comparison of different models for high damping rubber bearings in seismically isolated bridges," *Soil Dynamics and Earthquake Engineering* **104**, 329-345.

Yang, H., Yao, X.-F., Wang, S., Ke, Y.-C., Huang, S.-H., and Liu, Y.-H. [2018] "Analysis and inversion of contact stress for the finite thickness Neo-Hookean layer," *Journal of Applied Mechanics* **85**(10).

Yang, Y., and Chen, X. [2016] "Study of energy absorption and failure modes of constituent layers in body armour panels," *Composites Part B: Engineering* **98**, 250-259.